Evolution of the Southern Oscillation as Observed by the Nimbus-7 ERB Experiment

PHILIP E. ARDANUY

Research and Data Systems, Corporation, Lanham, MD 20706

H. LEE KYLE

NASA/Goddard Space Flight Center, Greenbelt, MD 20771

HYO-DUCK CHANG

STX Corporation, Hyattsville, MD 20784

(Manuscript received 8 December 1986, in final form 10 April 1987)

ABSTRACT

The Nimbus-7 satellite has been in a 955-km, sun-synchronous orbit since October 1978. The Earth Radiation Budget (ERB) experiment has taken approximately 8 years of high-quality data during this time, of which 7 complete years have been archived at the National Space Science Data Center. A final reprocessing of the wide-field-of-view channel dataset is underway. Error analyses indicate a long-term stability of 1% better over the length of the data record.

As part of the validation of the ERB measurements, the archived 7-year Nimbus-7 ERB dataset is examined for the presence and accuracy of interannual variations including the Southern Oscillation signal. Zonal averages of broadband outgoing longwave radiation indicate a terrestrial response of more than 2 years to the oceanic and atmospheric manifestations of the 1982–83 El Niño/Southern Oscillation (ENSO) event, especially in the tropics. This signal is present in monthly and seasonal averages and is shown here to derive primarily from atmospheric responses to adjustments in the Pacific Ocean. The calibration stability of this dataset thus provides a powerful new tool to examine the physics of the ENSO phenomena.

1. Introduction

The stable Nimbus-7 Earth Radiation Budget (ERB) dataset provides a useful new tool for examining the physics of the El Niño/Southern Oscillation (ENSO) event of 1982–83. The ERB experiment was launched aboard the Nimbus-7 satellite in October 1978 and has since accumulated 8 yr of solar and terrestrial irradiance measurements. An overview of the ERB observational system is presented by Jacobowitz et al. (1984) and of the calibration techniques by Kyle et al. (1984). In the processing, three sequential calibration methods were required to reduce the terrestrial irradiances. Thus, discontinuities were introduced in the data in June 1980 and in November 1983. In about 1 yr, however, a reprocessing of the dataset now underway will yield a long-term, consistently calibrated observational record for archival. In the interim, a tested set of corrections has been developed to facilitate interannual analyses of the entire dataset (Kyle et al., 1985). Error analyses indicate a long-term stability in the final products of better than 1% (Ardanuy and Kyle, 1986a).

The ERB parameter fields have been used to monitor the evolution of the 1982–83 ENSO event. Both the broadband outgoing longwave radiation (OLR) and albedo fields yielded information of particular interest (Ardanuy and Kyle, 1986b; Ardanuy et al., 1987). The question can now be asked: "Can the long-term stability of the data set be utilized to conduct observations of the Southern Oscillation during the period 1978–85?" Provided that the calibrations of the ERB channels have been accurately determined, the answer—we feel—is affirmative. The signal induced by the Southern Oscillation in the ERB measurements is unambiguous, and a 2+ year terrestrial recovery from the recent ENSO episode is clearly indicated.

2. Earth Radiation Budget measurements

Figure 1 illustrates a set of time series pairs of Earth Radiation Budget parameters, as derived from the Nimbus-7 ERB, for the data years 5, 6 and 7. The fifth year of data extends from 1 November 1982 through 31 October 1983 and includes the peak period of the 1982–83 ENSO event. Each time series is an integral across a hemisphere's tropics (e.g., 0° to 22.5°N; 22.5°S to 0°) and is a zonal and monthly mean. The parameters are also daily (diurnal) averages; thus, the dependency on the satellite's orbit has been removed.

The solar insolation is, to a first approximation, simply an astronomical function of time, modulated by the earth–sun distance and the solar declination.

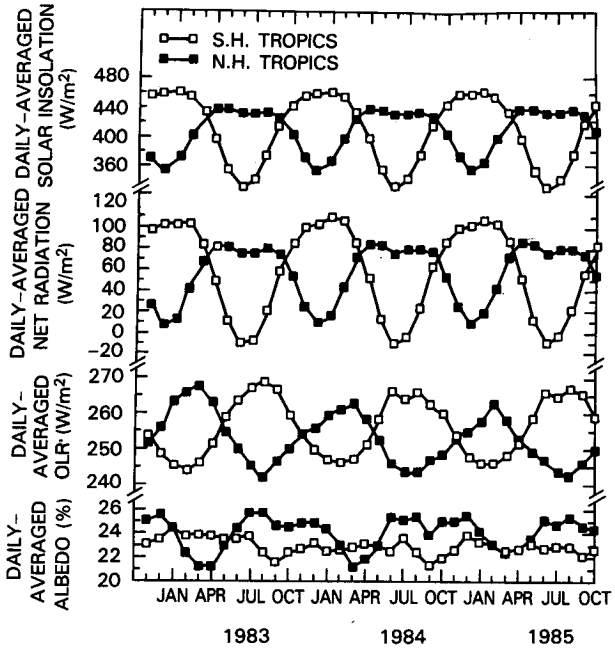

FIG. 1. Monthly averages of four Nimbus-7 ERB parameters zonally averaged over the Northern (0° to 22.5°N) and Southern (0° to −22.5°S) Hemisphere tropics for data years 5 (November 1982 to October 1983), 6, and 7. The parameters are the daily averaged solar insolation (W m^{-2}), net radiation (W m^{-2}), outgoing longwave radiation (W m^{-2}), and albedo (%).

As such, it can be directly computed without the need for observation. Clearly, the amplitude of the annual cycle in the Southern Hemisphere tropics is greater than for the north. This is due to the correlation of the two regulating factors. (For this area, the earth is closest to the sun when the sun is directly overhead, farthest from the sun when the sun is over the Northern Hemisphere.)

The net radiation (N) is defined as the combination of three terms: the incident solar insolation (S); the reflected solar insolation ($-AS$), where A is the earth's albedo; and the emitted outgoing longwave flux (L). Mathematically, the net radiation is defined as $N = (1 - A)S - L$. The insolation and net radiation curves are highly correlated; thus, the net radiation is driven to first order solely by changes in the solar insolation. Each tropical band absorbs the most radiation (incoming–outgoing) in its summer and the least in its winter. As one would expect, the amplitude of the annual cycle of the southern tropical net radiation is greater than for the north. In the northern tropics the net radiation is practically constant from April through September due to compensating contributions from the solar declination and the earth–sun distance. When the sun is the most directly overhead, it is the farthest away. When the net radiation is positive, either the earth (land, ocean, and atmosphere) is warming or compensating factors (such as horizontal transport) are acting.

A substantial phase difference exists between the OLR and either the solar insolation or the net radiation. The phase difference would be close to zero if the earth possessed no thermal inertia and simply warmed instantaneously in response to changes in solar forcing. Instead, however, the insolation and longwave radiation time series are practically 180° out of phase. The earth and its atmosphere are responding (in the tropics) to increases in solar insolation by increases in cloudiness—either increased cloud coverage, height, or optical depth. The cloud then radiates at a lower effective blackbody temperature than the corresponding clear-sky value, lowering the amount of longwave flux emitted to space. Note that the average albedo of the southern tropics does not vary a great deal. There are shallow minima associated with the maxima in the OLR, but the major cycles in the OLR are barely noticeable in the albedo. This would seem to indicate that seasonal changes in cloud type and cloud top altitude are also important. The observed changes in the OLR and net radiation might be explained by seasonal changes in the cirrus cloud fields and by seasonal changes in the relative importance of optically thick low and high clouds.

Figure 2 illustrates not only the pair of OLR time series for the tropics of each hemisphere, but also for the extratropics (poleward of 22.5°). A 180° phase difference between the tropics and extratropics is present. In the extratropics, more OLR is emitted during the hemisphere's summer and less during its winter. In the tropics, however, the opposite holds due to the effects of cloud forcing from the Asian monsoon and convection over the Amazon and Congo River valleys.

The difference between the two hemispheres is interesting. Such a hemispheric difference of OLR is presented in Fig. 3 for both the tropics and the full hemispheres. For the latter, a range of 25 W m^{-2} is noted in the monthly values, with the minima and maxima occurring approximately 1 month after the winter and summer solstices, respectively. In the tropics, the longwave difference curve, with an amplitude of over 40 W m^{-2}, reflects the movement of the intertropical convergence zone (ITCZ) and the monsoon system, with the greater Southern Hemispheric cloudiness in the southern summer (the convective regions over the Congo and Amazon River valleys and the Indonesian Archipelago) and the greater Northern Hemispheric cloudiness in the northern summer (India and Southeast Asia). In the signal the largest maximum occurs in the winter of 1982–83 and spring of 1983 and is directly related to the presence of the El Niño peak which occurred at that time.

All of the earth radiation budget parameters are important when considering the physics of the earth–atmosphere system. However, individual parameters, such as the OLR, sometimes give striking signals which can be used as an index of the state of complicated phenomena.

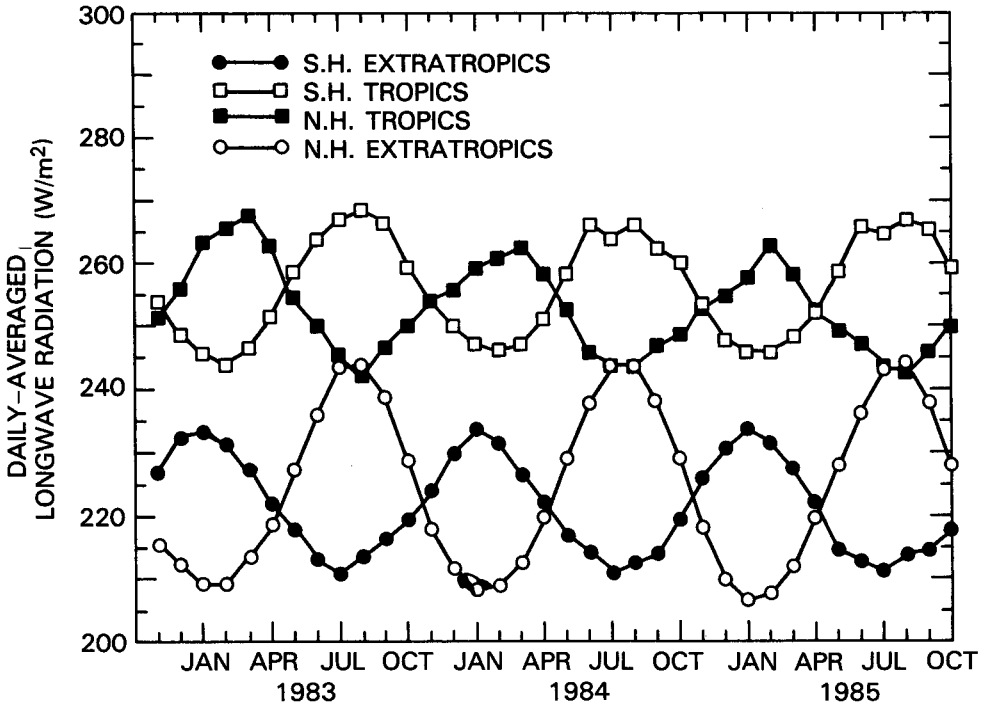

FIG. 2. Monthly averages of the daily averaged outgoing longwave radiation (W m^{-2}) zonally averaged over the tropics (0° to 22.5°) and extratropics (22.5° to 81°; due to the satellite's orbital inclination, the subsatellite track never passes poleward of 80.7° latitude).

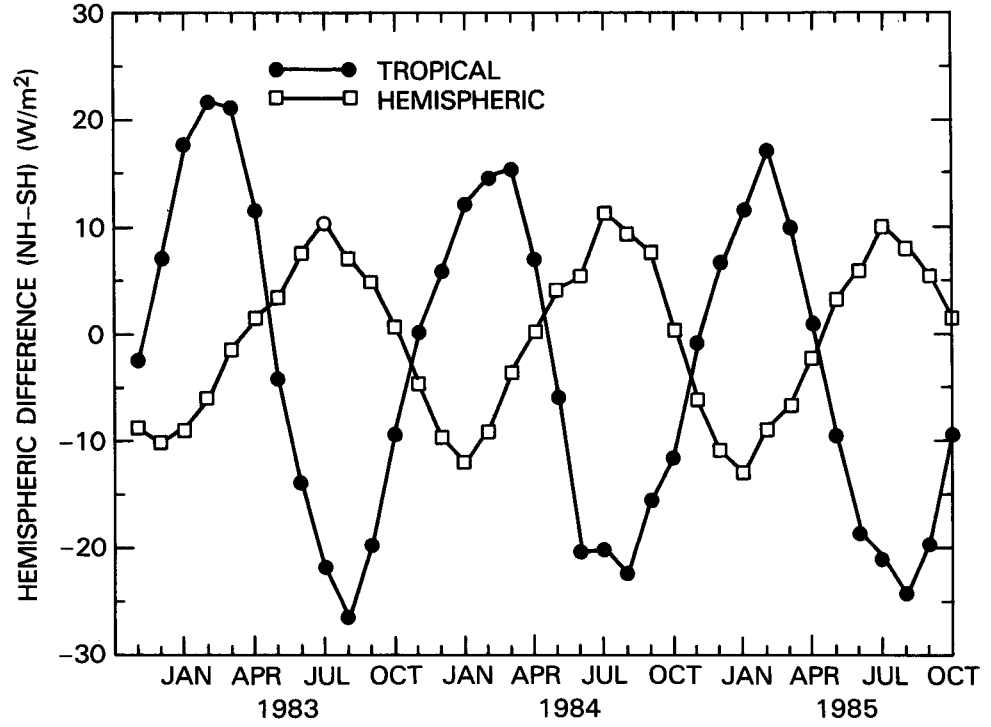

FIG. 3. Monthly averages of the daily averaged hemispheric and tropical differences of the outgoing longwave radiation (W m^{-2}).

3. Measures of the Southern Oscillation

A variety of measures are used to gauge the status of the Southern Oscillation, including the eastern equatorial Pacific Ocean sea surface temperature (SST), rainfall, 200 mb zonal winds, and the 850 mb trade winds. Also monitored are the station pressures at Darwin and Tahiti, and their difference, which provide a commonly used index of the Southern Oscillation Index (SOI). Each of the measures of the Southern Oscillation are meaningful because of the coupling that exists between the SST and the meteorological parameters during each El Niño.

It is also possible to use ERB parameters as a measure of the phase of the oscillation. Arkin et al. (1983) produced a "quick-look" atlas of the 1982–83 ENSO event which included the NOAA-7 AVHRR 11.5 μm-band OLR fields in addition to conventional meteorological parameter fields including the SST and the 850 mb and 200 mb wind fields. A decade of these narrowband measurements have been used to track the higher-frequency 40- to 50-day tropical mode (Lau and Chan, 1986; Weickmann, 1983). The OLR and albedo fields are each sensitive to cloudiness changes; the former, more responsive to cirrus presence and the latter, to lower-level optically thick clouds. In the presence of deep convection (or in its absence during a winter monsoon break), the OLR will give an indication of the convective intensity associated with the ENSO event. Thus, the equatorial OLR difference in the Pacific Ocean, east versus west of the date line will clearly illustrate the phenomenon (Ardanuy and Kyle, 1986b).

Each of the indices mentioned is useful as a diagnostic tool; of equal or greater interest would be a predictive indicator of the Southern Oscillation. Such a prognostic index could operate in two possible modes: it could indicate a predisposition towards the onset of an El Niño event, or it could suggest the absence of conditions requisite for such an episode. Physically, at least in part due to the time scale, the Pacific Ocean is believed to be intimately involved in driving the ENSO event. Therefore, an ideal prognostic index would be based on a measure of the oceanic thermal structure (e.g., the area-averaged depth or intensity of the thermocline). This, however, may not be necessary. We will show in this section that, while the Nimbus-7 ERB dataset may not provide the information sufficient to predict an El Niño, the stability of the dataset does permit a tracking of the Southern Oscillation signal over multiyear periods. Such a tracking may, in fact, be useful in providing remotely sensed estimates of the state of recovery of the Pacific Ocean following the conclusion of an ENSO occurrence. A new ENSO event may not be possible until an adequate readjustment occurs.

Figure 4a illustrates the hemispheric-averaged daytime and nighttime OLR for the month of April for the 7 yr between 1979 and 1985. For the 4 yr prior to

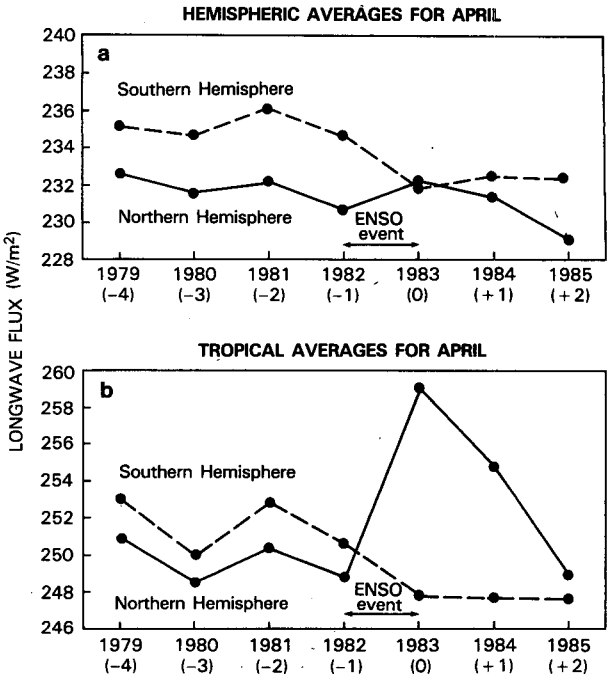

FIG. 4. (a) The hemispheric-averaged nighttime OLR and (b) the tropical-averaged (equatorward of 22.5°) nighttime OLR for April 1979–85 in W m^{-2}.

1983, the Southern Hemisphere OLR exceeds that of the north by 2 to 3 W m^{-2}. During the ENSO event the sign of the difference is reversed; 1 yr later, the sign of the difference is corrected and 1 W m^{-2} of the difference recovered. Two years after the episode, the hemispheric OLR difference resembles values in 1981 and in 1982 just prior to the onset. The variations are due to a variety of sources, including cloud variability, atmospheric water vapor content, SST, and air temperature. The former is perhaps the dominant forcing function. The change in sign during 1983 is caused by a southward displacement of cloudiness (Stowe et al., 1986). In 1984, one year after the conclusion of the ENSO event, hemispheric conditions had not fully recovered to the pre-ENSO climatology. The fact that the pre-ENSO characteristics of the OLR field only partially recovered a full year after the event suggests, not surprisingly, that the enormous amount of sensible heat lost by the Pacific Ocean during 1982–83 could not be replaced within a single year. Figure 4b illustrates the corresponding tropical OLR averages and clearly relates the effect of the migration of cloudiness out of the northern tropics during the ENSO event into the southern tropics and the northern midlatitudes.

A legitimate concern regarding the interpretation of the multiyear ERB signal as ENSO-related is the simultaneous presence of the stratospheric eruption cloud formed from the El Chichón volcano. However, it is easy to show that the resultant aerosol cloud did

not seriously affect the OLR measurements taken by the ERB experiment. First, the perturbations in the earth's albedo and OLR fields caused by the El Chichón stratospheric aerosols were small compared to those resulting from the ENSO. The El Chichón eruption in early April 1982 strongly increased the concentration of stratospheric aerosols. The increase was considerably larger in the Northern Hemisphere than in the Southern. These aerosols tended to decrease slightly the OLR signal and increase the albedo in the latitudes affected. The expected El Chichón signal should therefore have been small and of the opposite sign to the signal observed in Figs. 4a and 4b. These aerosol clouds were very visible to some narrow-field-of-view, narrow spectral band satellite sensors when viewing the cloud-free ocean (Matson, 1982). However, broad spectral band, wide-field-of-view (WFOV) sensors, which integrate clear and cloudy scenes, were not as sensitive to the aerosols. Analysis of the ERB wide-field-of-view data identified a significant El Chichón-related albedo increase in both the northern and southern polar regions. The strong ENSO albedo perturbations at lower latitudes masked any El Chichón signal. No definite El Chichón-caused OLR perturbations were identified at either middle or low latitudes (Ardanuy and Kyle, 1986c).

Figures 5a and 5b show, respectively, the SOI and a pair of indices defined by the Northern–Southern Hemisphere longwave flux differences of tropical and hemispheric zonal averages. Each index provides a "control" period prior to the onset of the ENSO event. The SOI is sensitive to the regional responses of the tropical surface pressure field, which in turn responds to longitudinal shifts in the associated oceanic and atmospheric parameters. As such, it recovers rapidly in mid-1983 at the end of the episode. In contrast, the zonal OLR indices indicate a terrestrial response of more than 2 years to the oceanic and atmospheric manifestations of the 1982–83 ENSO event.

A valid concern is the presence of noise introduced into the time series of the monthly averaged OLR measurements by variability unrelated to the Southern Oscillation signal. Undoubtedly, one such source of a spurious component in the time series is the tropical 40- to 50-day oscillation (Madden and Julian, 1971). To reduce the potential for error introduced by unwanted signals, the sample size is easily increased by averaging over an interval longer than 1 month. A 6-month (January to June) averaging interval was chosen for three reasons: first, the peak of the ENSO swing occurred in January 1983, so the 1983 average includes the period immediately following the intensification of the event; second, the 2-yr-plus recovery signal first noted in the time series of April measurements is present in each of these months; and, finally, any possible contamination of the desired multiyear signal due to synoptic variability or the well-known 40- to 50-day oscillation is reduced.

Table 1 represents the set of monthly and zonally averaged Northern–Southern Hemisphere tropical OLR differences for each of the 6 months, and the six-month average; the daytime and nighttime April and average time series are illustrated in Fig. 6. While the amplitude of the El Niño-related perturbation is clearly greater for April (11 to 12 W m^{-2}) than for the 6 month average (9 to 10 W m^{-2}), all four curves consistently exhibit six salient features:

1) There is relatively little variability in the differences prior to 1983.
2) All curves indicate a downward trend between 1980 and 1982.
3) Between 1982 and 1983 a major perturbation was introduced into the tropical OLR zonal averages.
4) A partial recovery from the anomalous 1983 amplitudes occurred by 1984.
5) The recovery continued between 1984 and 1985, with the two 6-month average curves reaching their 1980 levels.
6) Even by 1985, 2 yr after the peak of the 1982–83 ENSO episode, none of the curves have fallen as low as was registered in 1981 or 1982, just prior to the ENSO event.

4. Regional changes

In Ardanuy and Kyle (1986b), hereafter referred to as AK, the broadband OLR fields were examined for the period June 1980–October 1983. The monthly averaged, daytime WFOV observations were subjected to a resolution-enhancement process. The resultant spatially deconvoluted fields, and their anomalies, were then used to clearly describe the onset, intensification, and withdrawal of the 1982–83 ENSO episode. (A dataset containing the monthly, seasonal, and annual fields and their anomalies is now available in an atlas format.)[1] The OLR fields clearly demonstrated the global nature of the ENSO event. In particular, the following phenomena were identified by AK:

1) The drought region over Indonesia and northern Australia, with OLR anomalies reaching 65 W m^2 by January 1983.
2) The cloudy region over the equatorial central Pacific Ocean, with OLR anomalies attaining −88 W m^{-2} by January 1983; the OLR minimum was noted to extend eastward across the Pacific Ocean to Ecuador and northern Peru.
3) The drought/subsidence regions, at the ±20° latitudes, to the north and south of the mid-Pacific cloudy anomaly; the pair of areas contained positive OLR departures of 30 to 50 W m^{-2}, caused by enhanced sub-

[1] NASA, 1986: *El Niño and Outgoing Longwave Radiation: An Atlas of Nimbus-7 Earth Radiation Budget Observations.* NASA Ref. Publication RP-1163, 98 pp.

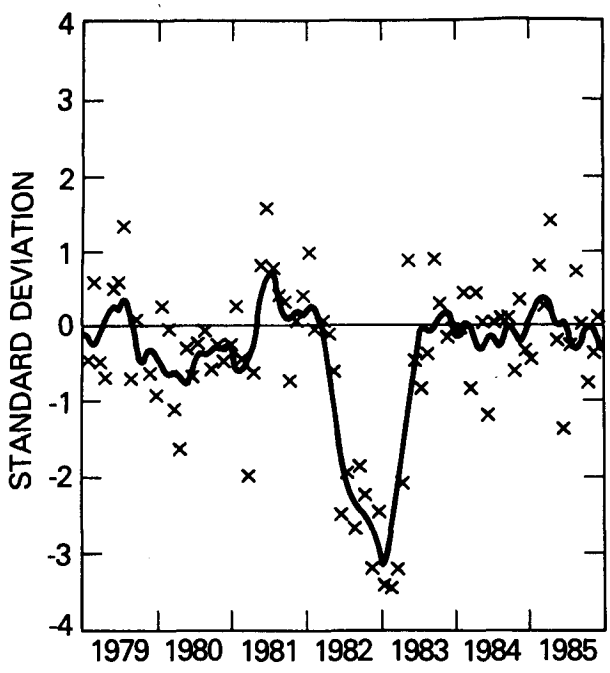

FIG. 5a. The Southern Oscillation Index as summarized from the February 1986 CAC Climate Diagnostics Bulletin.

sidence forced by the vigorous, thermally direct Hadley circulations accompanying the displacement of the cloudiness and resultant latent heat release.

4) The southward displacement of cloudiness and rainfall from northern to southern Brazil, between the late fall 1982 and early summer 1983.

5) A wave train of anomalies, extending from New Zealand across the equator to the southwest United States; the teleconnection pattern is centered about the equatorial convective anomaly, which appears to provide the forcing mechanism.

Two years of Earth Radiation Budget parameter data have now been processed since the completion of the ENSO event in mid-1983. As a result, the fields can be examined to identify regional changes in the data. An attempt can now be made to associate the observed changes in the measurements to a recovery, or partial recovery, from the episode.

The OLR fields, averaged over the 6-month period January–June, are illustrated in Figs. 7a–c for the years 1983, 1984, and 1985. The fields have been subjected to the identical resolution enhancement procedure as applied by AK to recover the true spatial amplitudes. The average for 1983 (Fig. 7a), of course, contains the El Niño-induced perturbations. These are most evident in the unusually strong subtropical high belts across the Pacific Ocean both north and south of the equator. The equatorial Pacific Ocean cloudiness displacement is also revealed, with an OLR minimum of 217 W m^{-2} noted at 150°W in 1983. The movement of the cloudiness over the Amazon River valley relative to that of the other 2 years is also apparent.

Figure 7d shows the 1-yr change in the OLR field (between 1983 and 1984); it is obtained by simply differencing Figs. 7a and 7b (1984 − 1983). A recovery in each of the five regions previously discussed is strikingly obvious: the winter monsoon cloudiness has unmistakably moved westward back to the Indonesian Archipelago from the central Pacific Ocean; the New Zealand–United States wave train anomaly has filled in, and with it the subsidence-forced anomalies in the

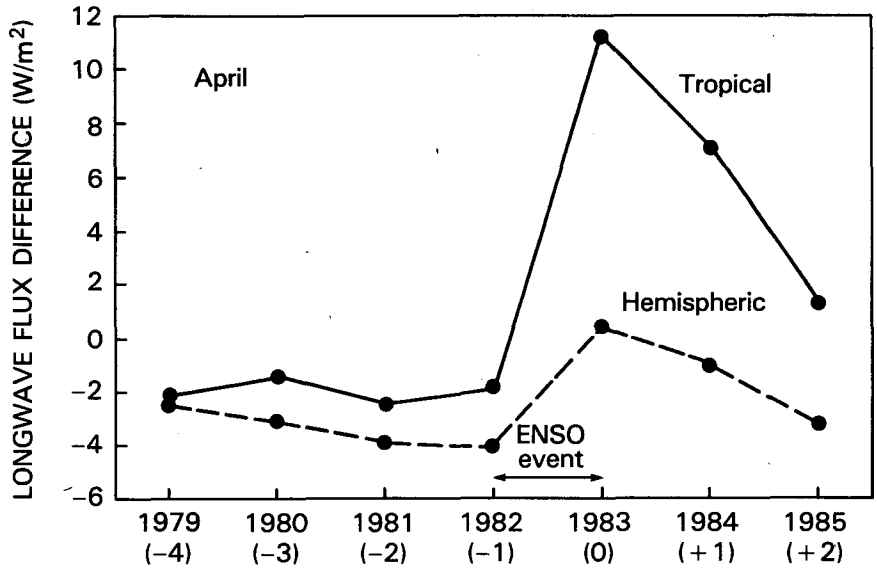

FIG. 5b. The Northern minus Southern Hemisphere and tropical nighttime OLR differences (W m^{-2}) for April 1979–1985.

TABLE 1. The set of monthly and zonally averaged Northern–Southern Hemisphere tropical longwave flux differences. These differences and their 6-month mean (W m^{-2}), as derived from the Nimbus-7 ERB experiment, highlight the strong swing in the Southern Oscillation between early 1982 and early 1983. As evidenced by the index in 1984, a complete recovery to the pre-ENSO conditions had not yet occurred. Only by 1985 had the signal decreased to a value characteristic (though still above the mean) of the 1979–82 background period.

	1979	1980	1981	1982	1983	1984	1985
				Nighttime			
Jan	15.0	17.7	16.9	12.3	18.1	12.8	12.7
Feb	12.9	19.1	16.3	14.3	22.3	15.7	18.0
Mar	10.3	10.2	9.2	8.1	21.5	16.1	10.7
Apr	−2.1	−0.4	−2.4	−1.8	11.2	7.1	1.3
May	−9.6	−13.2	−11.8	−15.4	−3.6	−5.0	−9.1
Jun	−21.3	−19.8	−17.2	−18.3	−12.1	−19.0	−17.6
Av	0.9	3.9	1.8	−0.1	9.6	4.6	2.7
				Daytime			
Jan	14.5	17.4	16.6	12.8	17.3	11.5	10.6
Feb	14.4	18.9	15.8	14.2	21.0	13.9	16.2
Mar	9.6	10.2	9.3	7.6	20.9	15.0	9.1
Apr	0.0	−1.4	−1.9	−1.7	11.7	7.1	0.5
May	−11.3	−13.2	−12.5	−17.5	−4.6	−6.8	−10.2
Jun	−24.1	−19.8	−19.0	−20.3	−15.5	−21.8	−19.7
Av	0.5	2.0	0.2	−0.8	8.5	3.2	1.1

Pacific subtropics; and the Brazilian convection has returned northward.

Though it appears from Fig. 7d that the ENSO features are completely removed by 1984, we know from the zonal-average time series shown earlier that this is not so, and that further substantial corrections occurred by 1985. To illustrate this second year, Fig. 7e presents the 1985–84 OLR difference. We expect that there will be anomalies present in any such difference (e.g., Short and Cahalan, 1983; Trenberth, 1984). Quite possibly, many of the maxima and minima present in this figure with amplitudes of 5 to 15 W m^{-2} are illustrative of this "typical" variability unrelated to the 1982–83 ENSO event. The notable exception is the −36 W m^{-2} feature present in the central Pacific Ocean north of the equator, extending from New Guinea to the Gulf of Mexico. Further, a ring of positive anomalies fully surrounds this central feature, covering most of the Pacific Ocean northward from 10°S, most of the Indian Ocean, the Indonesian Archipelago, and the

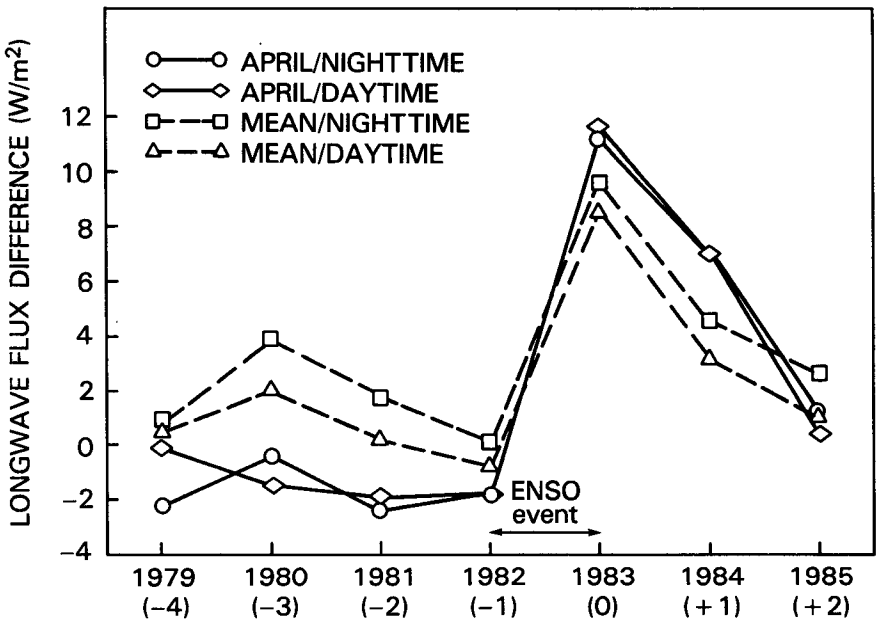

FIG. 6. The northern minus southern tropical daytime and nighttime OLR difference time series (W m^{-2}), for April and for the 6-month (January through June) average, for 1979–85.

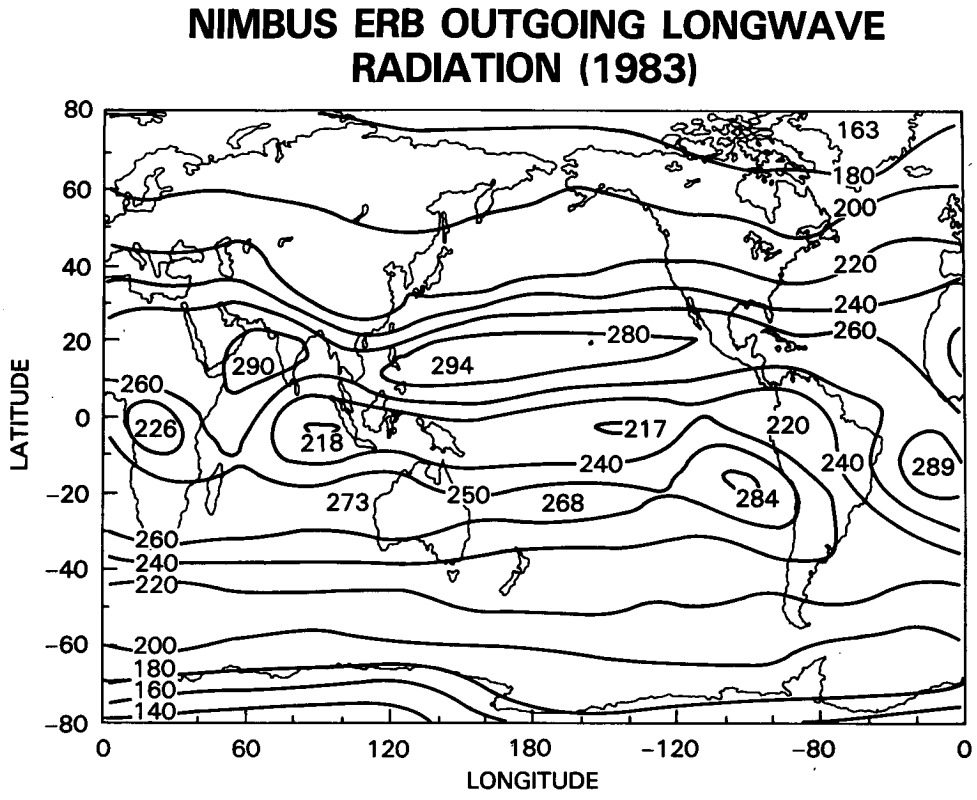

FIG. 7a. The 6-month (January through June) average of the Nimbus-7 ERB WFOV daily averaged outgoing longwave radiation (W m^{-2}), after resolution improvement, for 1983 (ENSO).

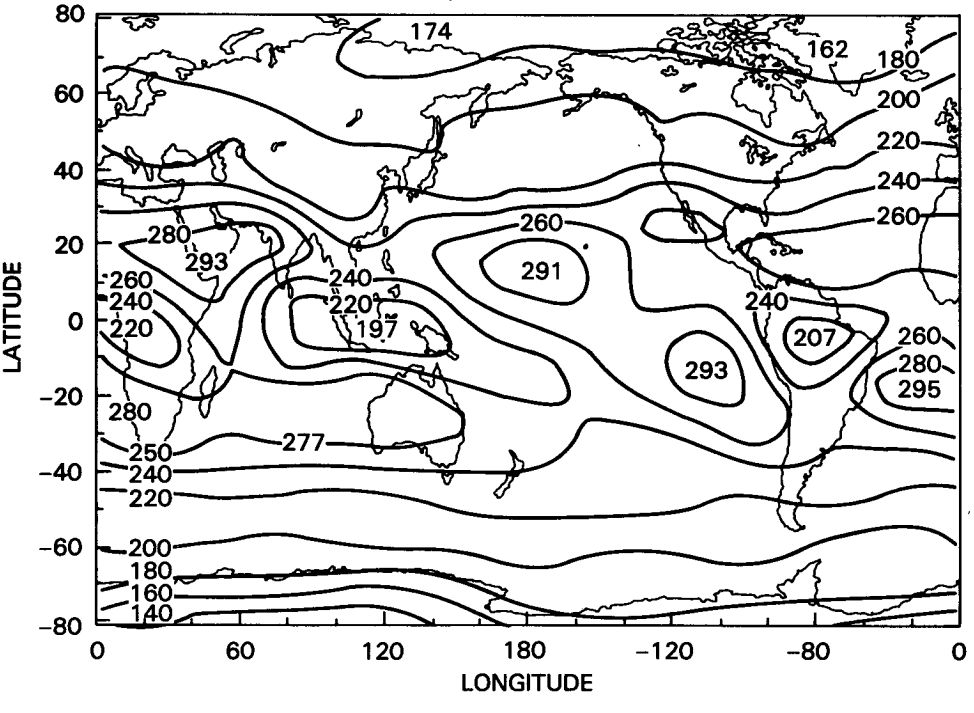

FIG. 7b. As in Fig. 7a except for 1984 (ENSO plus 1 yr).

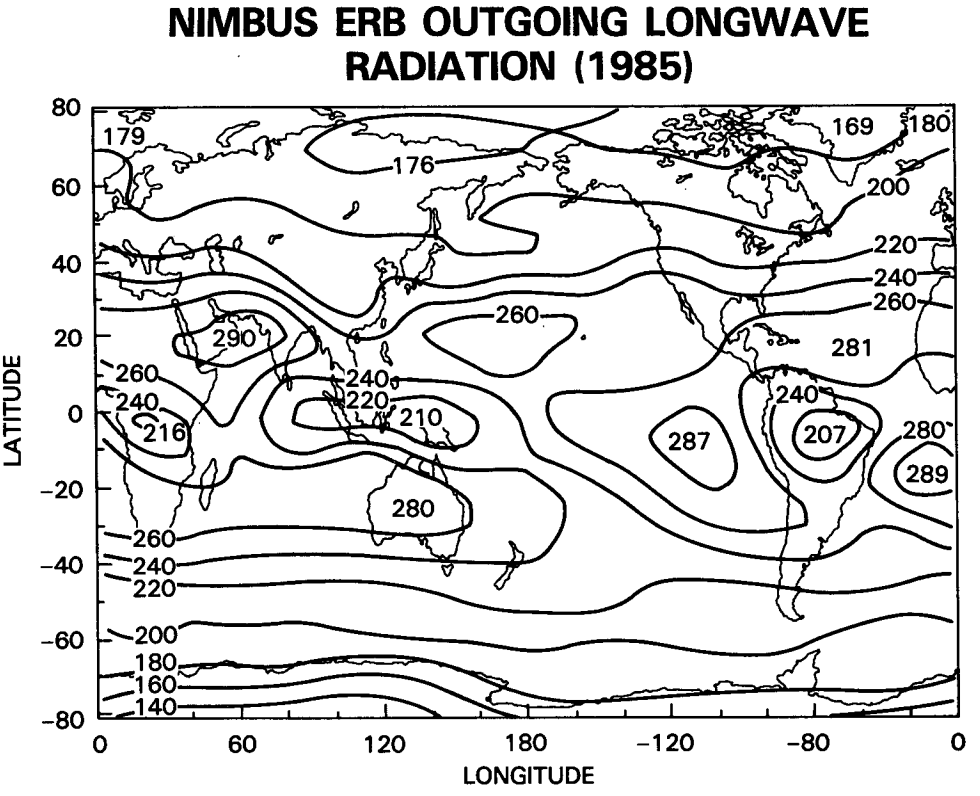

FIG. 7c. As in Fig. 7a except for 1985 (ENSO plus 2 years).

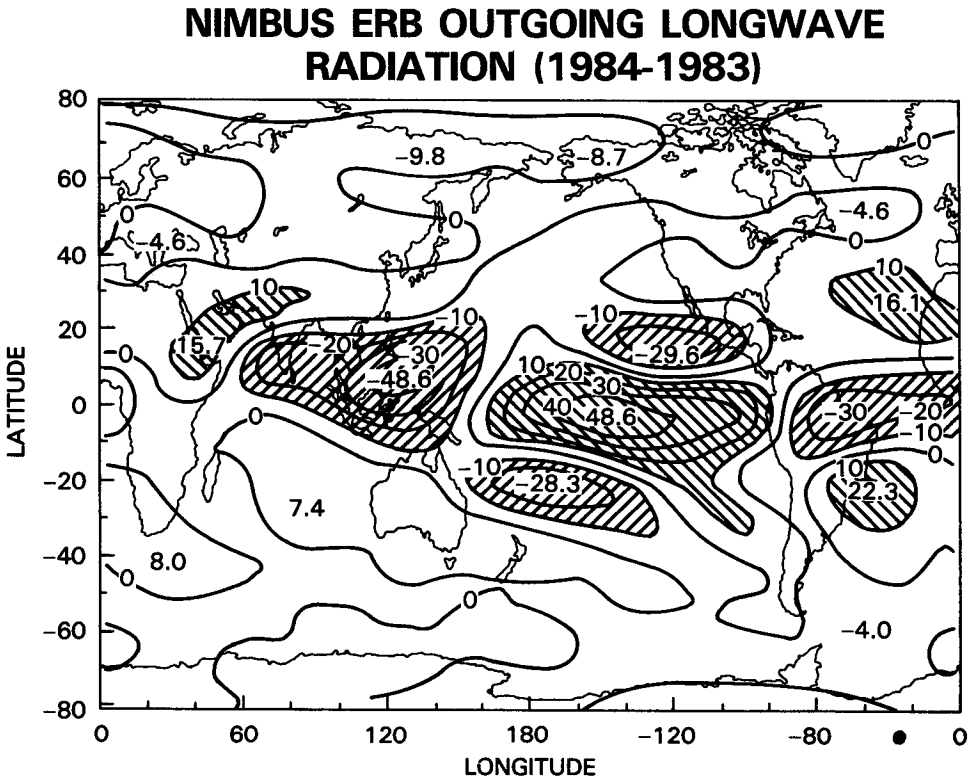

FIG. 7d. The difference between the 6-month averages of daily averaged outgoing longwave radiation (W m^{-2}) for 1983 and 1984 (1984 − 1983).

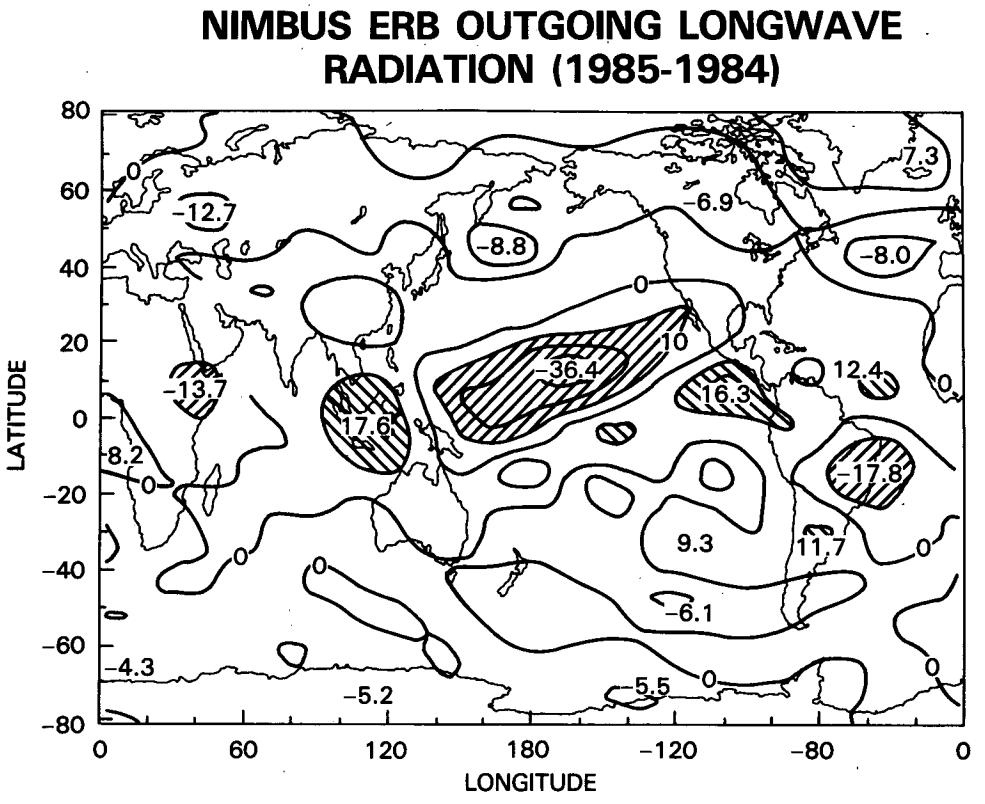

FIG. 7e. As in Fig. 7d except for 1984 and 1985 (1985 − 1984).

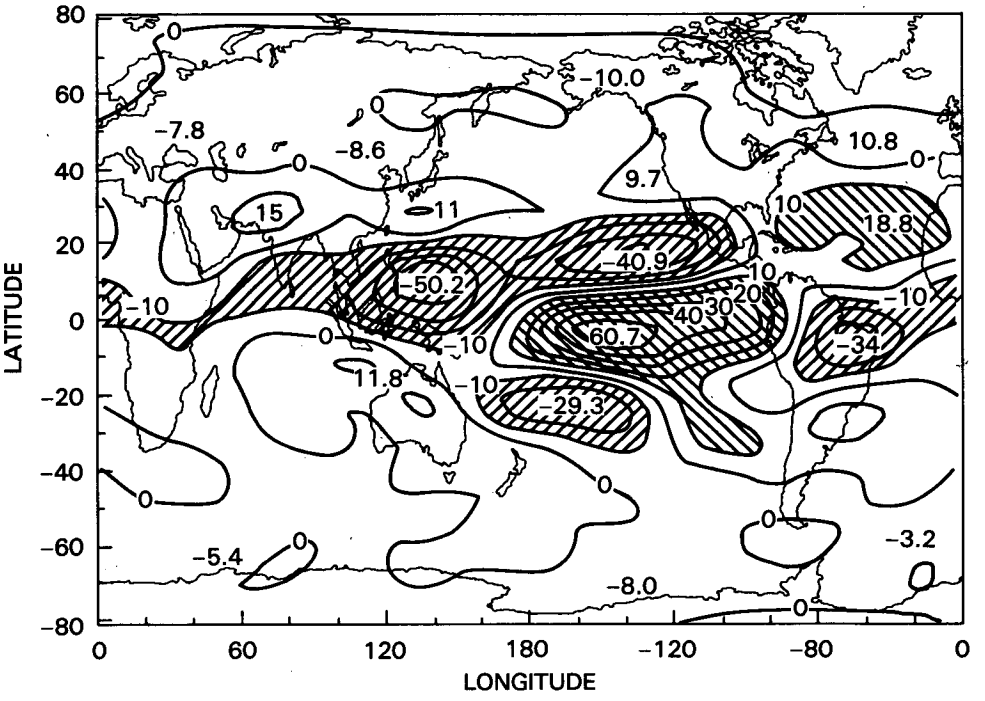

FIG. 7f. As in Fig. 7d except for 1983 and 1985 (1985 − 1983).

United States. Other differences are present locally over the eastern Amazon River valley, Indonesia, and in the Pacific Ocean off the west coast of Central America.

When the two differences are combined (Fig. 7f), the difference in the averaged OLR fields between 1983 and 1985 is obtained. Relative to the 1-yr (1984) recovery, several significant modifications have occurred. Most notably, in the equatorial Pacific Ocean the positive OLR differences increase in magnitude from 50 to 60 W m^{-2}. To the north, in the eastern Pacific subtropics, the negative difference intensifies from −30 to −40 W m^{-2}. The effect of these two features primarily produces the 2-yr recovery time scale evident in the zonally averaged time series.

5. Concluding remarks

In AK, the OLR fields derived after resolution improvement from the Nimbus-7 ERB experiment were used to document the presence of ENSO-induced quasi-stationary planetary-scale tropical and midlatitude patterns. The El Niño year and the two previous years of data were employed. The dataset has now been extended by 2 years to encompass 7 years of coverage, with processing well underway into the eighth year. A consistent calibration set is being applied to yield the first long-term, broadband, continuous Earth Radiation Budget dataset in history. The stability that has been attained permits the application of this product to many research areas, particularly towards the analysis of contemporary climate variation and change.[2] The stability of the calibration of this 8-year measurement record gives us a powerful new tool to examine the physics of the ENSO phenomena.

The next El Niño episode following the 1982–83 event began in late 1986 and reached a peak in 1987. The present study, based on the Nimbus-7 longwave radiation data, shows that conditions reminiscent of the 1981–82 (pre-El Niño) period were being approached, though not yet reached, by 1985 (Fig. 6).

The ENSO event of 1982–83, and indeed the entire set of measurements during the period 1979–85, is only a single realization of the ENSO cycle. Further, the particular El Niño episode sampled in this study is an extreme example of this phenomena—probably the most pronounced of the past century (Rasmusson and Wallace, 1983). Therefore, one may not wish to generalize the findings reported here as being representative of all ENSO cycles.

Although data are still being taken, the lifetime of the Nimbus-7 ERB experiment is limited to, at most, another few years. Earth Radiation Budget data from the follow-on ERBE experiment (Barkstrom, 1984) can be used, perhaps in conjunction with continued Nimbus-7 ERB data, to track the El Niño of 1986–87 and possibly the next ENSO event when it occurs.

[2] Details on the archived ERB data are found in Kyle et al. (1985).

Acknowledgments. The authors wish to thank Dr. Eugene Rasmusson, the editor, and the anonymous reviewers for their critical and helpful comments which resulted in a substantial strengthening of this manuscript. Also to be acknowledged is the assistance of Mr. Richard Hucek and Mr. Mitchell Weiss of Research and Data Systems, Corporation for their generous assistance in preparing Figs. 7a–f, and Ms. Brenda Vallette for her word processing assistance, which was of the highest quality.

REFERENCES

Ardanuy, P. E., and H. L. Kyle, 1986a: Climate variability as observed by Nimbus-7 ERB. Extended abstracts of the *Sixth AMS Conf. on Atmospheric Radiation,* Williamsburg, Amer. Meteor. Soc., 284–289.

——, and ——, 1986b: El Niño and outgoing longwave radiation: Observations from Nimbus-7 ERB. *Mon. Wea. Rev.,* **114,** 415–433.

——, and ——, 1986c: Observed perturbations of the earth's radiation budget: A response to the El Chichón stratospheric aerosol layer? *J. Climate Appl. Meteor.,* **25,** 505–516.

——, ——, R. R. Hucek and B. S. Groveman, 1987: Improvement of the earth radiation budget products and consideration of the 1982–83 El Niño event. *J. Geophys. Res.,* **92,** 4125–4143.

Arkin, P. A., J. D. Kopman and R. W. Reynolds, 1983: *1982–83 El Niño/Southern Oscillation Event Quick-Look Atlas.* Climate Analysis Center, W/NMC52, Washington, DC, 80 pp.

Barkstrom, B. R., 1984: The Earth Radiation Budget Experiment (ERBE). *Bull. Amer. Meteor. Soc.,* **65,** 1170–1185.

Jacobowitz, H., H. V. Soule, H. L. Kyle, F. B. House and the Nimbus-7 ERB Experiment Team, 1984: The Earth Radiation Budget (ERB) experiment: An overview. *J. Geophys. Res.,* **89,** 5021–5038.

Kyle, H. L., F. B. House, P. E. Ardanuy, H. Jacobowitz, R. H. Maschhoff and J. R. Hickey, 1984: New in-flight calibration of the Nimbus-6 and -7 ERB WFOV radiometers. *J. Geophys. Res.,* **89,** 5057–5076.

——, P. E. Ardanuy and E. J. Hurley, 1985: The status of the Nimbus-7 Earth Radiation Budget data set. *Bull. Amer. Meteor. Soc.,* **66,** 1378–1388.

Lau, K. M., and P. H. Chan, 1986: The 40- to 50-day oscillation and the El Niño/Southern Oscillation: A new perspective. *Bull. Amer. Meteor. Soc.,* **67,** 533–534.

Madden, R. A., and P. Julian, 1971: Detection of a 40- to 50-day oscillation in the zonal wind in the tropical Pacific. *J. Atmos. Sci.,* **28,** 702–708.

Matson, M., 1982: Radiative effects of the El Chichón volcanic eruption: Preliminary results concerning remote sensing. NASA TM 84959, W. R. Bandeen and R. S. Fraser, Eds., NASA/Goddard Space Flight Center, 87 pp.

Rasmusson, E. M., and J. M. Wallace, 1983: Meteorological aspects of the El Niño/Southern Oscillation. *Science,* **222,** 1195–1202.

Short, D. A., and R. F. Cahalan, 1983: Interannual variability and climate noise in satellite-observed outgoing longwave radiation. *Mon. Wea. Rev.,* **111,** 572–577.

Stowe, L. L., P. P. Pellegrino and P. H. Hwang, 1986: Spatial and temporal characteristics of global cloud cover as observed from the Nimbus-7 satellite. Extended abstracts of the *Sixth AMS Conf. on Atmospheric Radiation,* Williamsburg, Amer. Meteor. Soc., 99–102.

Trenberth, K. E., 1984: Some effects of finite sample size and persistence on meteorological statistics. Part II: Potential predictability. *J. Atmos. Sci.,* **112,** 2364–2379.

Weickmann, K. A., 1983: Intraseasonal circulation and outgoing longwave radiation modes during northern winter. *Mon. Wea. Rev.,* **111,** 1838–1858.